Experiment proposal: ERDA measurements for the determination of He and Ar distributions in nuclear ceramics

G. Velisa[a], D. Pantelica[a] ,L. Thomé[b], C. Nita[a] ,A. Debelle[b], L. Vincent[b], N. Scintee[a], P. Ionescu[a], A. Declémy[c], J. Jagielski[e,f]

[a] National Institute for Physics and Nuclear Engineering - "Horia Hulubei", *407 Atomistilor St., Magurele-Ilfov, P.O. Box: MG-6, 077125, ROMANIA*

[b] Centre de Spectrométrie Nucléaire et de Spectrométrie de Masse, UMR8609, Univ. Paris-Sud 11, Bât.108, 91405 Orsay, France

[c] Laboratoire de Physique des Matériaux, UMR6630, CNRS-Université de Poitiers, BP 30179, F-86962 Futuroscope-Chasseneuil Cedex, France

[d] Institute of Electronic Materials Technology, Wolczynska 133, 01-919 Warszawa, Poland

[e] The Andrzej Soltan Institute for Nuclear Studies, 05-400 Swierk/Otwock, Poland

Abstract

Crystalline oxide ceramics (particularly, zirconia and spinel) are promising matrices for nuclear waste immobilization and/or transmutation. The behavior of implanted ions and of radiation damage is a very important issue in the qualification of nuclear matrices. Ion beams provide very efficient tools for such an evaluation. He and Ar depth profiles will be measure by ERDA using high-energy Cu ions.

1. Scientific motivation

Due to its excellent physico-chemical properties, such as an elevated melting temperature, a relatively high thermal conductivity, and a good radiation resistance, crystalline oxide ($MgAl_2O_4$ and ZrO_2) has received considerable attention as potential matrix for the transmutation of actinides[1–5]. For many applications such as the safe and long term disposal of radioactive waste and the development of inert fuel matrices for actinide transmutation, it is of prime importance to study the production and recovery of radiation damage and the behavior of inert gases (He, Ar) in this type of materials. Such a study may be performed by introducing the species to be confined via ion implantation and by following the structural evolution upon subsequent thermal treatments[6].

The depth distribution of implanted He atoms and the modifications of the He depth profile upon thermal treatments are then generally determined via nuclear reaction analysis, for instance by using the (d,p) reaction on ^{3}He. However, this latter technique suffers a few drawbacks such as time consuming measurements and rather low-accuracy data. A possibility to extract helium profiles in a simpler way is to perform elastic recoil detection analysis (ERDA) with high energy heavy ions, which allows the simultaneous measurement of a wide range of elements, including hydrogen[7]. The first use of a (ΔE - E_r) ionization chamber in elastic recoil detection measurements was reported in [8]. The use of heavy ion beams offers significant advantages. However, one of the experimental problems using ΔE - E_r detectors is the simultaneous detection of the full range of recoil atoms ejected by the heavy ion beams, since all low-mass recoils have almost identical velocity and also exhibit a wide spread of ranges in the detector. Often two or more gas pressures are required to detect both low-mass and heavy recoil atoms. Simultaneous measurement of many elements is highly desirable, since in this case no other parameters such as collected charge are needed for the analysis of the data. In IFIN at the Nuclear

Physics Department we started almost 18 years ago to use our 8.5 MV tandem accelerator for material analysis [2]. An ERDA beam line equipped with a dedicated target chamber has been installed. A compact ΔE - E_r telescope(Fig. 1) consisting of a gas (ΔE) ionization chamber and a silicon (E_r) detector has been developed.

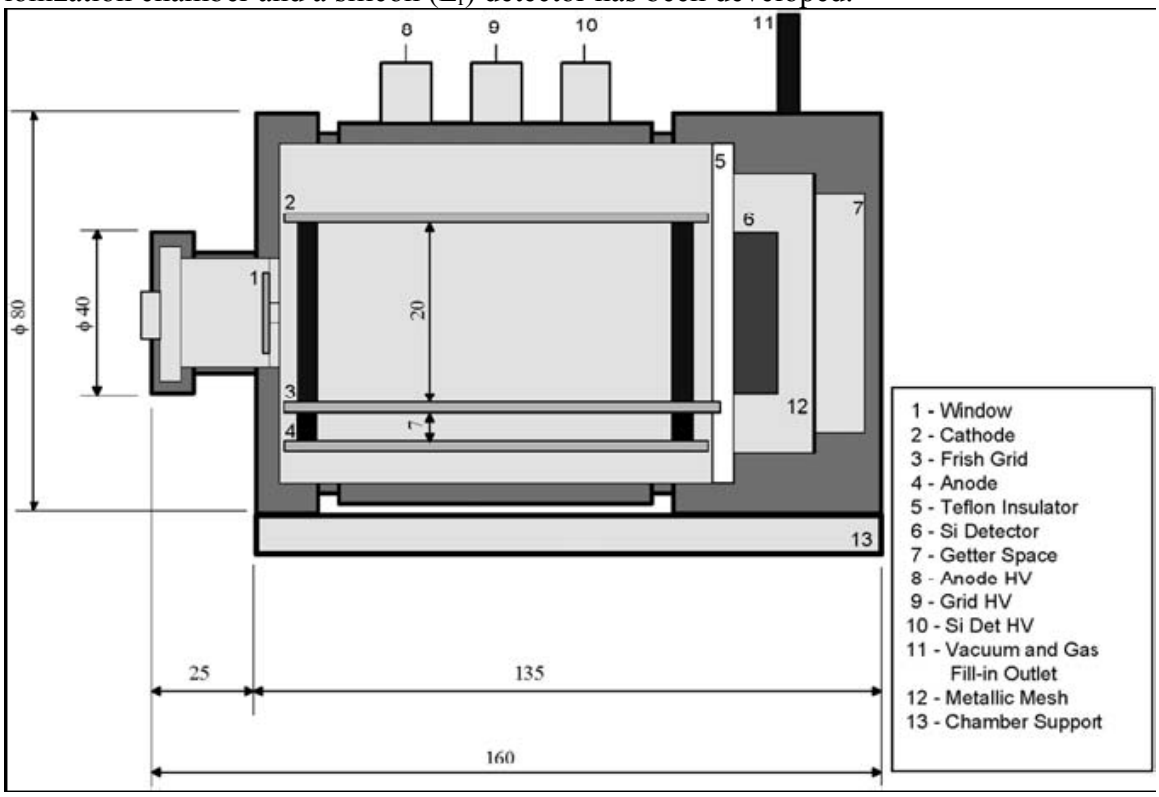

Fig. 1. The ΔE - E_r telescope

A prerequisite for the precise quantitative evaluation of the ERDA data is the correct energy calibration of the data. The data acquisition system is used to register all multiparametric events during the experiment; data are registered in list mode on disk for further processing. The total two-parameter (DE _ Er) spectra are reconstructed after the experiment. For each element present in the sample, the total energy spectrum (histogram) was built using the PAW [99] program. However, to reconstruct the total energy spectrum, the energy calibration for both the ionization chamber and the Si detector should be determined. An example of our data for one of the runs is shown in Fig. 2, in the form of calculated energy versus measured pulse-height. The lines represent the best fit with a second order polynomial to the data points.

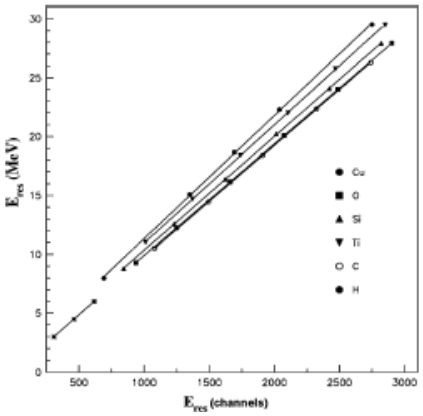

Fig. 2. Calibration curves energy versus pulse height measured for the Si detector.

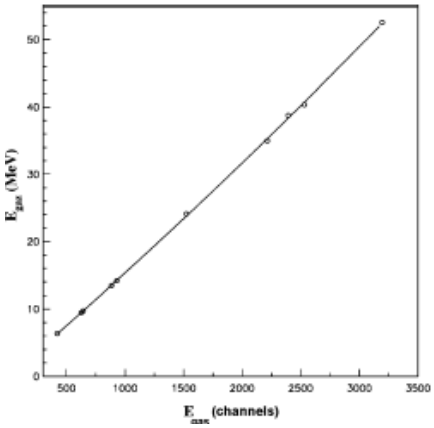

Fig. 3. Calibration curve (energy versus pulse height amplitude) measured for the ionization chamber.

The slope increases systematically from light to heavy ions. The PHD increases with increasing ion energy and charge. For our detector the PHD is considerable, even for relatively light ions like ^{12}C, ^{16}O and ^{28}Si. For the same ions elastically scattered from the Au foil we measured two parameter ΔE - E_r spectra at different gas pressures and ion energies. Using calculated energies for the elastically scattered ions, corrected for energy loss in the gold foil and in the mylar window, we get the total energy of the ions when entering the ionization chamber. The residual energy E_r can be determined using the calibration curves measured for different ions. The difference between the total energy and residual energy represents the energy loss in the gas. So, an energy calibration of the ionization chamber can be accomplished. In Fig. 3 we present the calibration data for the ionization chamber, measured in one of the runs.

The procedure followed to extract the information about the composition of a sample form experimental data taken in ERDA measurements consists in three steps:

– getting the calibration coefficients from calibration runs;

– build the total experimental energy spectra (histograms) for each sample, and for each element present in the sample (Fig. 4);

– adjust the parameters describing the sample composition so that the theoretical spectra reproduce the experimental ones(Fig. 5).

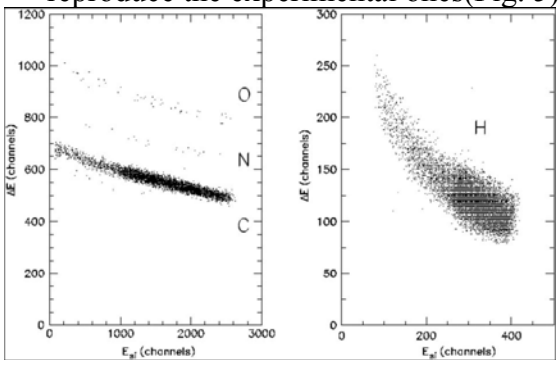

Fig. 4. ΔE - E_r spectra measured with a 63Cu beam at 80 MeV incident on a DLC sample.

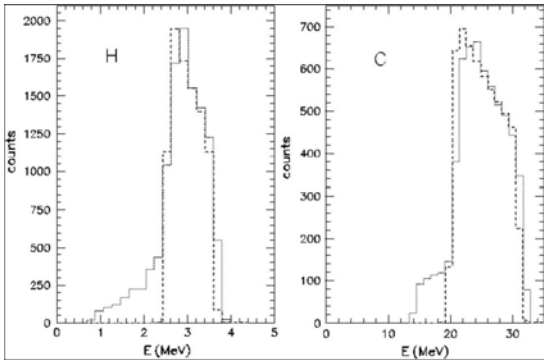

Fig. 5. Total energy spectra of the main components of the DLC sample.

Fig. 6 shows the ΔE - E_r spectra corresponding to high and normal amplification of a $MgAl_2O_4$ single crystal sample implanted with 30 keV He ions at a fluence of $2x10^{16}$ at/cm^2. The spectra were taken with a 80 MeV ^{63}Cu beam. The H recoils from the sample surface and He recoils are seen in the identification matrix corresponding to high amplification of the ΔE signal. The identification matrix corresponding to normal amplification shows O, Mg and Al, the components of the spinel. Because the surface of the sample was covered with a thin carbon layer in order to avoid charging effects, the carbon signal from the surface is also present.

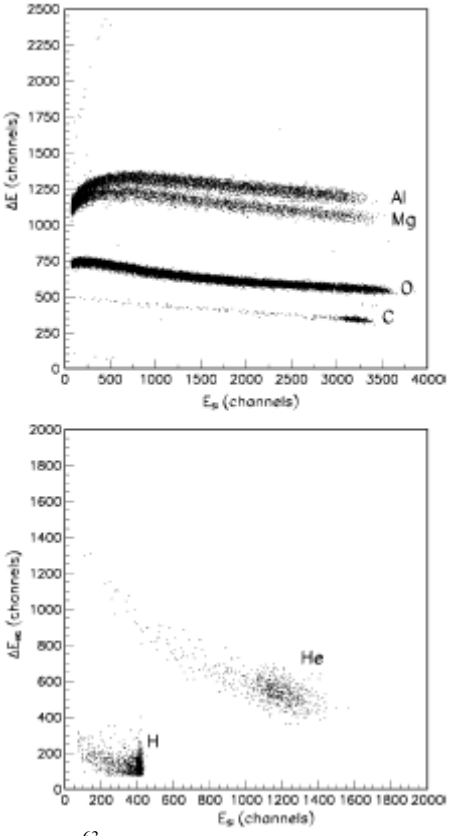

Fig. 6. ΔE - E_r spectra measured with a ^{63}Cu beam incident on a $MgAl_2O_4$ single crystal implanted with 30 keV He ions at a fluence of 2 x10^{16} at/cm^2

ERDA measurements are very important to determine the He depth distributions before and after the thermal treatment and to correlate them with defect profiles. An example: the experimental results show that low-energy (30 keV) He implantation in YSZ leads to the formation of a thin damaged layer. Actually, the damage is weak, as indicated by the low accumulated damage fraction (~0.3 at the damage peak) and confirmed by the weak diffuse X-ray scattering. After annealing at 800°C, a surprising large increase of the disorder level is observed. This result may signify that the thermal energy brought during this treatment did not induce a defect recovery but on the contrary led to a more damaged structure. Actually, TEM reveals the formation of fractures (see Fig. 10(b)) which are essentially located at the maximum of the damage distribution. These fractures may explain both the strain relaxation and the large increase of the diffuse X-ray scattering (Fig.9). He bubbles are also clearly observed on the TEM

micrograph (Fig. 10(b)). It is likely that the small He-vacancy clusters generated during implantation grew upon annealing to form these He bubbles. Furthermore, these bubbles are present from the end-of-range of implanted He ions up to the crystal surface. This may explain why the implanted layer is found to be highly damaged up to the surface (see RBS/C results of Fig. 8b)), contrary to what was observed after implantation. The presence of these He bubbles up to the crystal surface may be tentatively attributed to He (or more likely to He-vacancy clusters) migration upon annealing, in conclusion it is very important to correlate the implantation and defect profiles.

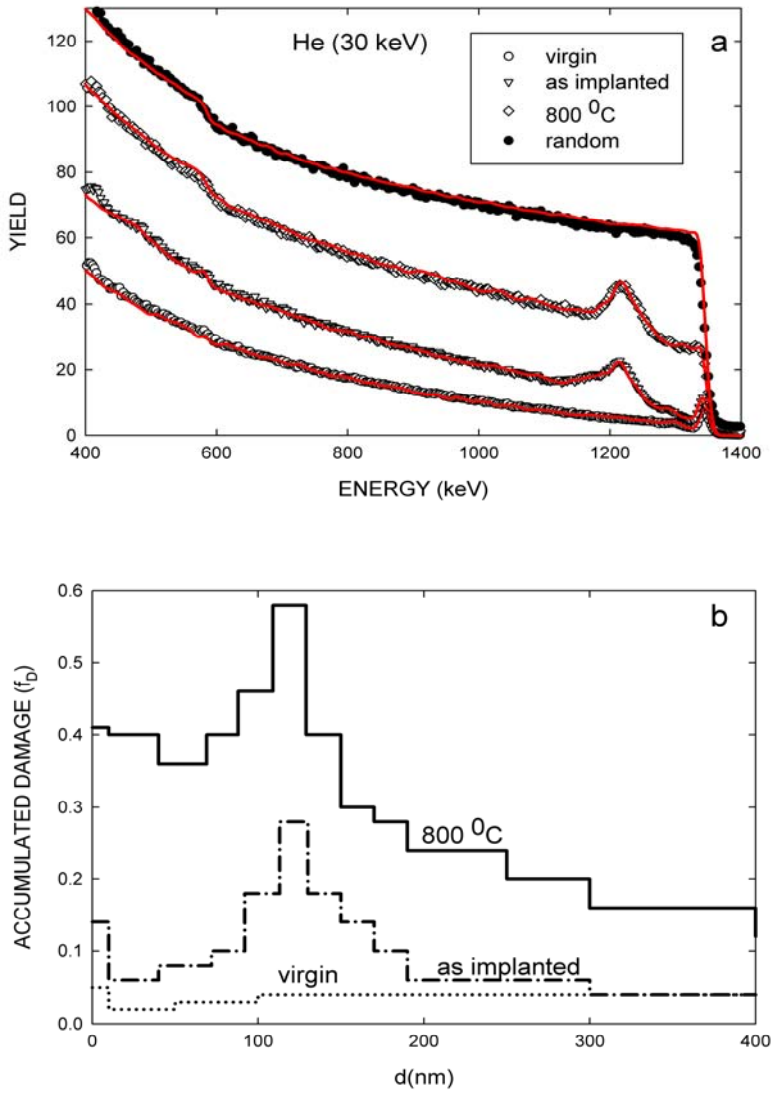

Fig. 1. Top: RBS spectra recorded in random (filled symbols) and <100> axial (open symbols) directions on YSZ single-crystals implanted at RT with 30 keV He ions at $5x10^{16}cm^{-2}$ and annealed for 1 h at 800°C. Solid lines are fits to RBS spectra with MC simulations. Energy of the analyzing 4He beam: 1.6 MeV. Bottom: Damage depth profiles in the Zr sublattice of YSZ extracted from the analysis of RBS spectra recorded on crystals implanted with 30 keV He ions and annealed at 800 ^{0}C.

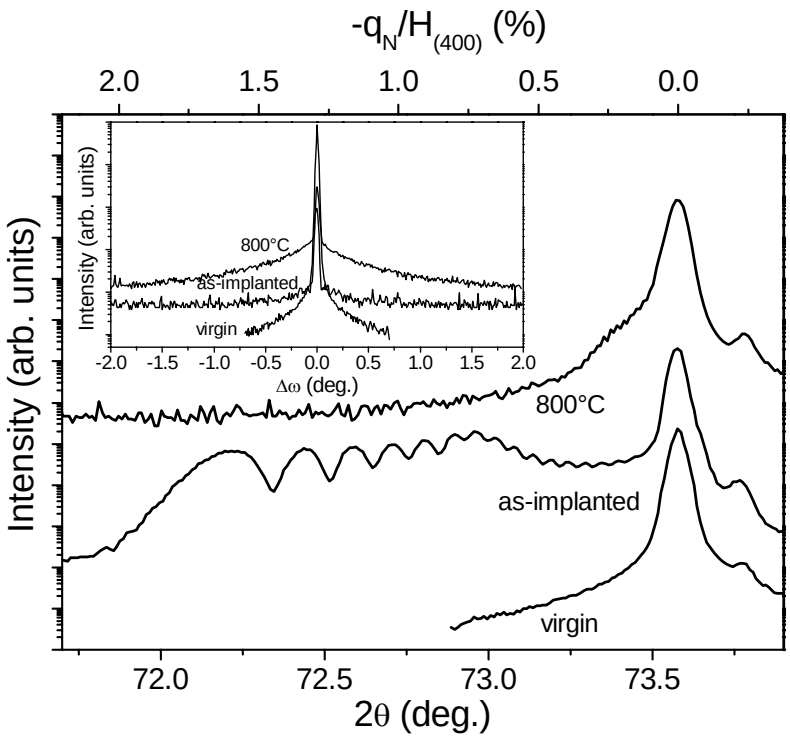

Fig. 2: X-ray scattered intensity distribution in the vicinity of the (400) Bragg reflection on YSZ crystals implanted at RT with 30 keV He ions at $5x10^{16}cm^{-2}$ and annealed for 1 h at 800°C. The XRD curve of a virgin crystal is also displayed.

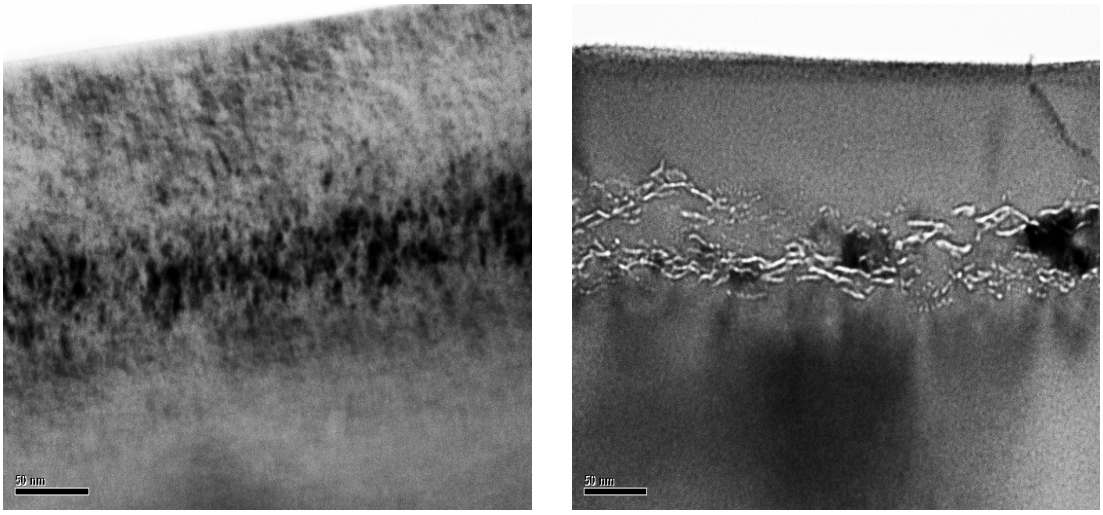

(a) **(b)**

FIG. 3: TEM micrographs obtained from (a) a YSZ single-crystal implanted with 30 KeV He ions at RT at $5x10^{16}$ cm^{-2}, and (b) subsequently annealed at 800°C**.**

The realization of this experiment will give to our group the possibility to accomplish our task from the Collaboration Agreement between CSNSM-Orsay (France) and NIPNE-Bucharest, entitled: "**Characterization of nuclear ceramics using Ion Beam Analysis (IBA) technique**" and also will give the possibility to realize the scientific report of **Program Grants No. 71-103.** It will give the opportunity to finish my thesis, titled: "***Macroscopic and microscopic modifications induced by irradiation in thin films of AII-BVI compounds and nuclear ceramics***". By determining the He depth distributions before and after the thermal treatment, we can correlate He profiles to damage depth distributions. The results concerning the microstructural modifications in nuclear ceramics implanted with He and Ar ions have been presented at: 15th Radiation Effects in Insulators (poster), 2010 MRS Spring Meeting (poster), E-MRS 2010 Spring Meeting (oral presentation) and ION 2010 (poster) conferences. I consider that the results already obtained are very important. In consequence we published 2 ISI paper(G. Velisa, A. Debelle, L. Vincent, L. Thomé, A. Declémy, D. Pantelica, J. Nucl. Mater. 402 (2010) 87-92 si G. Velisa, A. Debelle, L. Vincent, L. Thomé, D. Pantelica, A. Declémy,Nucl. Instr. and Meth. B (2010), *accepted*.) and 1 is submitted at JNM.

In conclusion, the only missing results are the He depth distributions before and after the thermal treatment and if this experiment will succeed we will achieve scientific base to publish more papers in important ISI journals.

2. Beam time estimation and beam characteristics

In order to obtain a reliable energy calibration for the Si detector, which exhibits a pulse height defect when used with heavy ions [10], the pulse height versus energy response will measure for a variety of ions (from ^{1}H to ^{63}Cu) at energies ranging from 2 to 30 MeV. The ions were obtained by elastic scattering of the corresponding beams on a thin Au target. Spectra measured without gas in the ionization chamber and without the mylar window will be used to investigate the pulse height versus energy relationship for different ions. In conclusion, based on our previous measurement, we ask for a number of 7 days of beam time (21 shifts). ^{63}Cu ions should be accelerated to 80 MeV.

3. Experimental equipment

We will use the ΔE - E_r telescope from the 4th beam line. The electronic set-up which will be use is fairly conventional. The energy loss signals and the residual energy signal will fed to three ADCs that were parts of a multiparameter acquisition system based on a PC, where the data will be stored.

References

[1] F.W. Clinard Jr., G.F. Hurley, L.W. Hobbs, D.L. Rohr,R.A. Youngmann, J. Nucl. Mater. 122–123 (1984) 1386.

[2] S.J. Zinkle, J. Am. Ceram. Soc. 72 (1989) 1343.

[3] K.E. Sickafus, A.C. Larson, N. YU, M. Nastasi, G.W. Hollenberger, F.A. Garner, R.C. Bradt, J. Nucl. Mater.219 (1995) 128.

[4] M. Burghartz, H.J. Matzke, C. Le´ger, G. Vambene`pe, M.Rome, J. Alloys Compd. 271–273 (1998) 544.

[5] Hj. Matzke, V.V. Rondinella, T. Wiss, J. Nucl. Mater. 274(1999) 47.
[6] G. Velisa, A. Debelle, L. Vincent, L. Thomé, D. Pantelica, A. Declémy,Nucl. Instr. and Meth. B (2010), *accepted*.
[7] D. Pantelica et all. Nucl. Instr. and Meth. B 249 (2006) 504–508
[8] M. Petrascu, I. Berceanu, I. Brancus, A. Buta, M. Duma, C. Grama, I. Lazar, I. Mihai, M. Petrovici, V. Simion, Nucl. Instr. and Meth. B 4 (1984) 396.
[9] CERN, PAW Manual Version 1.14, Application Software Group,Computing and Network Division, CERN, Geneva, Switzerland, 1992.
[10] J.J. Grob, Theses, Strasbourg, 1971.